

VALIDATION OF THE MERIS ATMOSPHERIC CORRECTION OVER OCEAN USING AERONET

Ouahid AZNAY^(1,4), Richard Santer^(1,2) and Francis Zagolski^(1,3)

⁽¹⁾ ADRINORD, Association pour le Développement de la Recherche et de l'Innovation dans le bassin du Nord-Pas-de-Calais, 2 rue des Canoniers, F59000, Lille – FRANCE.

E-mail: Santer.Richard@yahoo.fr

⁽²⁾ ULCO, Université du Littoral Côte d'Opale, MREN, 32 avenue Foch, Wimereux, F62930 – FRANCE.

⁽³⁾ PARBLEU Technologies Inc., 79 Veilleux street, St Jean-sur-Richelieu (QC), J3B-3W7 – CANADA.

E-mail: Francis_Zagolski@yahoo.ca

⁽⁴⁾ C-S Systèmes d'Information, ZAC de la Grande Plaine, F31506, Toulouse - FRANCE.

E-mail: ouahid.aznay@c-s.fr

ABSTRACT

We propose an atmospheric approach to validate the atmospheric corrections over water. The sensor is MERIS and the ground-based instrument is the CIMEL radiometer in AERONET. The idea is to evaluate all the atmospheric functions required in the atmospheric corrections. The inputs are provided by AERONET after inversion of the optical measurements [1], the radiative transfer code used for this study is the SOS code [2]. The MERMAID database in AAOT is used to illustrate this new concept for validation.

1 INTRODUCTION

Validating the atmospheric corrections (ACs) mainly over coastal water areas requests an “*atmospheric*” approach. Both the atmosphere and the water body present very complex and variable optical properties. By looking at water surfaces in a cloud-free scene acquired with an optical sensor such as MERIS, we observe more likely the pattern of the ocean colour rather than the spatial variability of the aerosols. Therefore, why not to use the atmospheric optical measurements rather than the marine optics?

It is clear that the atmospheric corrections cannot be validated only through *in situ* measurements of the aerosol optical thicknesses (AOTs). Validation of the atmospheric corrections passes also by a well estimate of the atmospheric scattering components. The diffuse atmospheric transmittance can be directly provided by the sky radiance measurements. The aerosol reflectance at the top of the atmosphere (TOA) can be estimated with the acquisition of the sky radiances at the same scattering angle as for the sensor/view geometry, in order to well predict the primary scattering. The introduction of the multiple scattering requires more with the aerosol phase function (APF) and the AOTs. The full protocol of the validation scheme for the atmospheric correction over ocean is described hereafter.

Both *in situ* measurements and MERIS level-2 data extracted from MERMAID over the AAOT site (Acqua Alta Oceanographic Tower, Venice - Italy) is employed to illustrate the methodology in a direct comparison between marine reflectances derived from the MERIS ESA Ground-Segment (MEGS) processor and extracted with an atmospheric correction based on the characterization of the inherent optical properties (IOPs) of the aerosols at the time of MERIS overpass.

2 THE STANDARD APPROACH

The MERMAID database focuses on the retrieval of the water reflectance. Nevertheless, the spatio-temporal variability of the watercolour in coastal areas makes difficult this approach. Complementary to this, the retrieval of the AOT is an indicator of the potential performance of the atmospheric correction. In MERMAID, the comparison was initially brought on the AOT in the NIR region. More recently, MERMAID included the visible part of the spectrum. The comparisons on the AOT at 560, 665 and 865 nm stresses, first an important bias (about 40 % at 865 nm, 13 % at 665 nm and about 20 % at 560 nm) and second a large dispersion of the measurements (Figure 1). The latter results from the large dispersion observed in the APF as reported in a companion proceeding [3].

As we already evoked it, current official MERIS algorithm overestimates the retrieved AOT over coastal waters especially in the NIR region. It can be verified on Figure 1.

The AOT describes the extinction that gives the attenuation of the light propagation in the atmosphere on the direct-to-direct path. The atmospheric correction involves the scattering functions that are not measured. Consequently we use the sky radiance measurements.

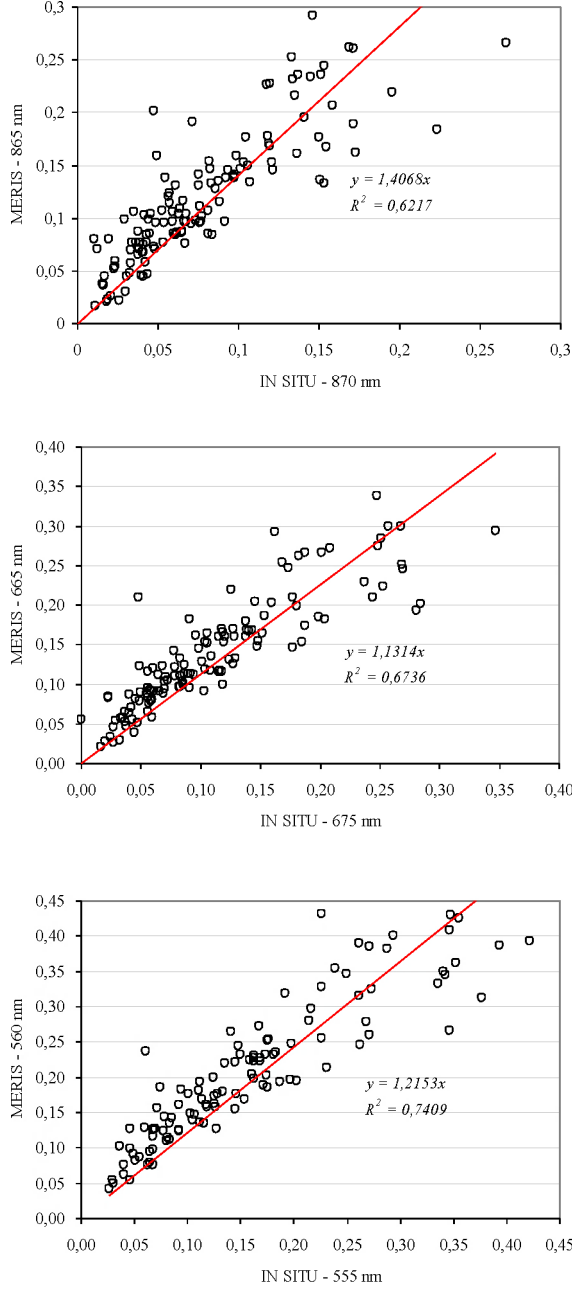


Figure 1: AOTs at 560, 665 and 865 nm collected over AAOT: comparison between in-situ and MERIS.

3 A NEW APPROACH FOR VALIDATION

In our approach, we do not validate the gaseous correction or the sunglint correction. The gaseous correction combines radiative transfer computations and knowledge of the gas content. For the sunglint, we need to rely on a wave slope distribution model and the wind speed as ECMWF auxiliary data. All these corrections are a matter of *a priori* choices and not the result of the interpretation of the MERIS

measurements. Therefore, we do not validate the latter and we use the TOA reflectance after gas and sunglint correction, ρ_{gcs} , as provided in MERMAID database.

The 5S formalism is used to perform the atmospheric correction:

$$\rho_{TOA} = \rho_{atm} + \rho_w T(\theta_s)T(\theta_v) \quad (1)$$

ρ_{TOA} , ρ_{atm} and ρ_w are respectively, the reflectance of water target at TOA, the intrinsic atmospheric reflectance and the *in situ* water reflectance, and $T(\theta_s)$, the total (direct + diffuse) downward atmospheric transmittance corresponding to the ratio of the BOA to TOA irradiances for the solar zenith angle (θ_s) measured over a dark water body including the *Fresnel* reflection. $T(\theta_v)$, the total upward atmospheric transmittance, represents (following the principle of reciprocity) the ratio of the BOA to TOA irradiances for the view zenith angle (θ_v) measured over a dark water body ignoring the *Fresnel* reflection.

AERONET network provides AOTs at 440 nm (B_2), 675 nm (B_7) and 870 nm (B_{13}) and the APF at the same wavelengths. The barometric pressure and the wind-speed are auxiliary data for MERIS. Using these inputs, the successive order of scattering (SOS) code is used first to compute ρ_{atm} and $T(\theta_s)$, and second to calculate $T(\theta_v)$ in the three MERIS reference bands. These runs are also completed for the pure *Rayleigh* case with ρ_R , $T_R(\theta_s)$ and $T_R(\theta_v)$. Combining these 2 sets of computations, we get ρ_{aer} , $T_{aer}(\theta_s)$ and $T_{aer}(\theta_v)$ also in the three MERIS reference bands. A spectral interpolation in *Log-Log* is then achieved to obtain ρ_{aer} , $T_{aer}(\theta_s)$ and $T_{aer}(\theta_v)$ in all the MERIS bands.

In addition, the direct sun glint component is also computed with the attenuation on the direct-to-direct path as provided by the CIMEL extinction measurements.

MERMAID also provides in all these MERIS bands ρ_R , ρ_{aer} , $T(\theta_s)$ and $T(\theta_v)$ for the comparisons.

Moreover, by using the 5S formalism and the derived CIMEL atmospheric functions (by SOS RTC), the water reflectance can be also predicted as:

$$\rho_w = \frac{\rho_{TOA} - \rho_{ATM}}{T(\theta_s)T(\theta_v)} \quad (2)$$

The latter will be compared to the MERIS product. We depict in Figure 2 the flowchart describing these comparisons:

Upper left: The AERONET aerosol IOP and the barometric pressure and wind-speed are used to compute the atmospheric functions in the three reference spectral bands.

Lower left: The SOS derived aerosol optical properties (AOPs) are interpolated at the MERIS nominal wavelengths. Then, by using the 5S formalism, the water reflectance is computed and compared both with the MERIS L2 product and the in-situ data reported in MERMAID.

Upper right: The MERIS derived AOPs are used to compute ρ_{aer} for comparison with the SOS predicted value.

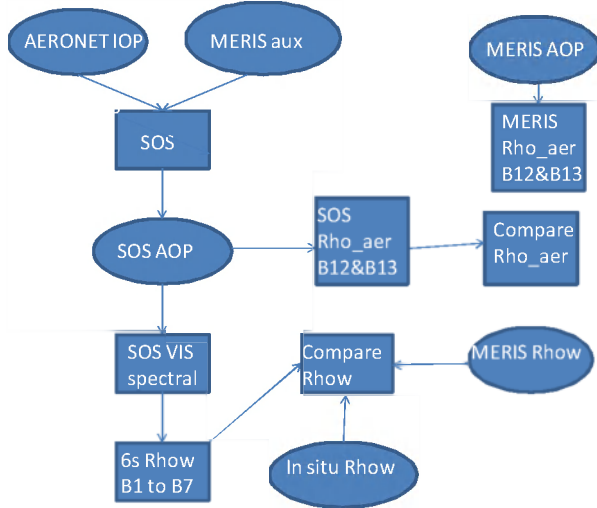


Figure 2: Flowchart describing the methodology for the atmospheric functions comparisons.

4 COMPARISONS ON THE ATMOSPHERIC FUNCTIONS

4.1 Extinction and direct sunglint correction

As we mentioned it previously, we do not want to validate the sun glint correction, but we know that there is a bias: the attenuation on the direct-to-direct path only accounts for the *Rayleigh*. Ignoring the presence of the aerosols overestimates the correction. It is an important issue, because on the 1079 matchups on the AAOT, 420 of them are contaminated but the so-called medium glint for which the AC is applied.

The first step is to compute the amount of reflectance $d\rho_G$ we have to add on the TOA signal when including the aerosol extinction. The *Cox and Munk* [4] wave slope distribution is associated to the wind speed proposed in the MERIS auxiliary data. This extinction is computed in all the MERIS bands from the CIMEL AOT measurements.

Let's assume that this additional reflectance $d\rho_G$ in B_{12} and B_{13} corresponds to an increase of the aerosol

reflectance ρ_a . In the primary scattering, we can relate it to an increase of the AOT as:

$$d\tau_a = \frac{\tau_a d\rho_g}{\rho_a} \quad (3)$$

Figure 3 reports $d\tau_a$ corresponding to the new AOT minus the old one, versus the old sun glint reflectance with no atmosphere. The increase of τ_a is quite white, similar between B_{12} and B_{13} .

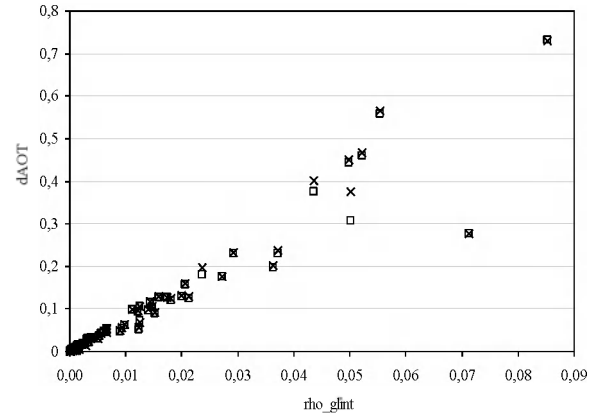


Figure 3: Increase of the AOT in B_{13} (squares) and B_{12} (crosses) versus the sunglint reflectance when accounting for the aerosols in the attenuation.

Therefore the new Angström coefficient is smaller as illustrated in Figure 4. In MERMAID, we have access to the AOT in B_5 , B_{12} and B_{13} . We readjust these values with the additional sun glint reflectance to obtain new AOT values.

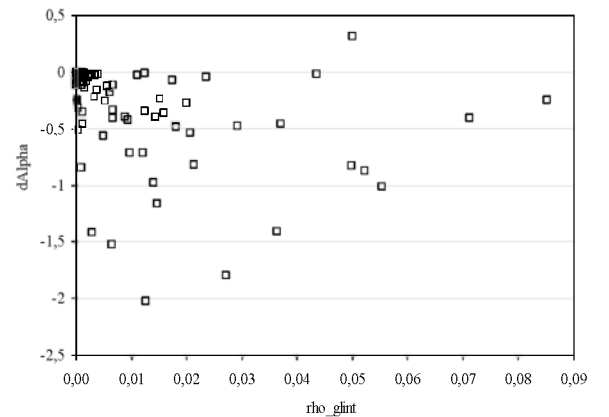


Figure 4: Same as Figure 3 but on the decrease of α (computed between B_{12} and B_{13}).

With these new AOTs, we recomputed the total transmittance and the new ρ_{aer} as:

$$d\rho_a = \frac{\rho_a d\tau_a}{\tau_a} \quad (4)$$

Figure 5 gives the increase of ρ_{aer} versus ρ_{glint} . At the end, on the atmospheric parameters, we transform the over correction of the sun glint into an increase of τ_a and ρ_{aer} . Conversely we have a decrease of the transmittance (T).

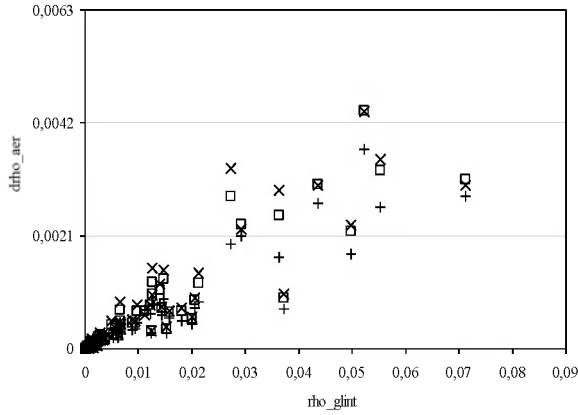


Figure 5: Increase of the aerosol reflectance resulting of the new correction of the sunglint. Results are for B₁ (stars), B₄ (squares) and B₇ (crosses).

We use Eq. 2 to obtain the new values of the water reflectance. Simply ρ_{gc} is increased by $d\rho_G$ and the new atmospheric functions are introduced in Figure 6.

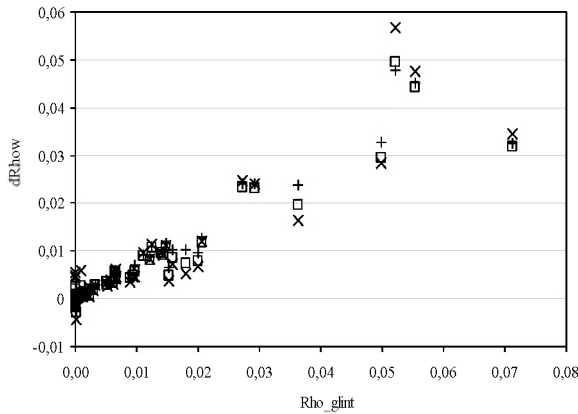


Figure 6: same as Figure 5 but for the water reflectance.

4.2 Validation of the aerosol reflectance

The SOS aerosol reflectances values are computed using as inputs the AERONET AOTs and APFs at 440, 675 and 870 nm. We can directly compare them with

the MERIS ones in B₂, B₇ and B₁₃. Results displayed in Figure 7 stress that the MERIS aerosol reflectance in B₁₃ is correctly retrieved. When considering Figure 1, this result confirms the MERIS aerosol reflectance and indicates that the MERIS APF is underestimated as suggested in [3]. In B₂ MERIS seems to slightly overestimate the aerosol reflectance.

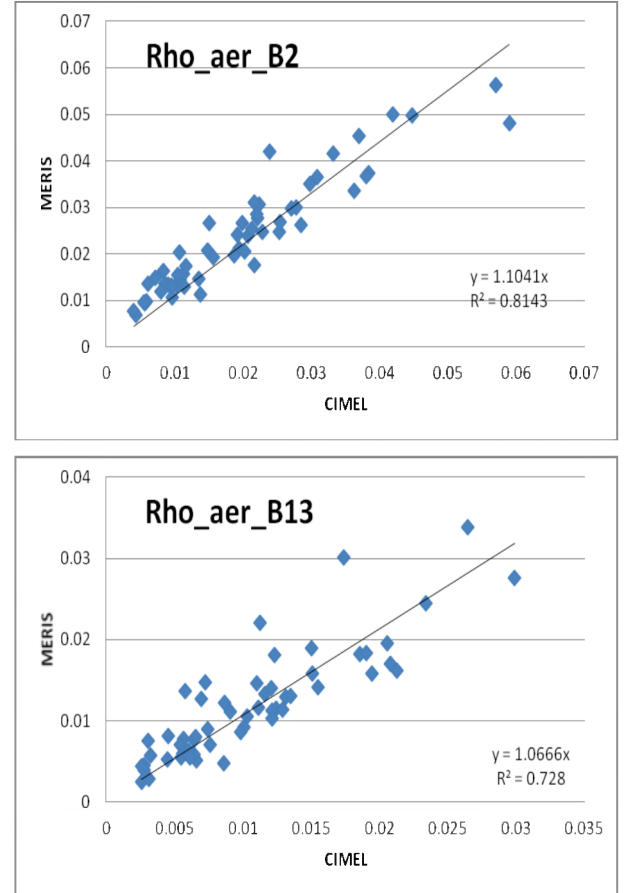


Figure 7: Aerosols reflectance at 865 nm (bottom) and 443 nm (upper): comparison between MERIS and SOS simulations.

In terms of atmospheric correction, the key issue is to be able to predict the aerosol reflectance in the visible part of the spectrum from its NIR determination. This is the reason why we force the CIMEL ρ_{aer} to be equal to the MERIS ρ_{aer} in B₁₃. Doing so, we see in Figure 8 that MERIS predicts correctly ρ_{aer} in B₂.

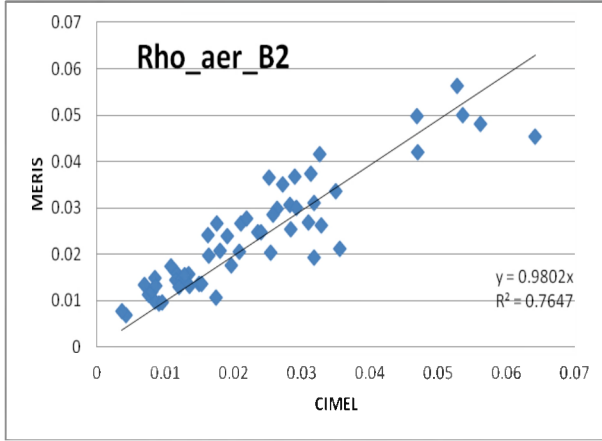


Figure 8: Same as in Figure 7 but we forced the agreement in B_{13} on ρ_{aer} between MERIS and AERONET.

4.3 Validation of the atmospheric transmittance

The atmospheric transmittance in the visible domain is mostly attributed to the *Rayleigh* scattering. We isolated the aerosol transmittance from our comparison between the MERIS and SOS estimates based on the AERONET measurements (Figure 9).

It clearly appears that our prediction of the attenuation by the aerosols is a little higher than what MERIS predicts simply because MERIS overestimates the AOTs.

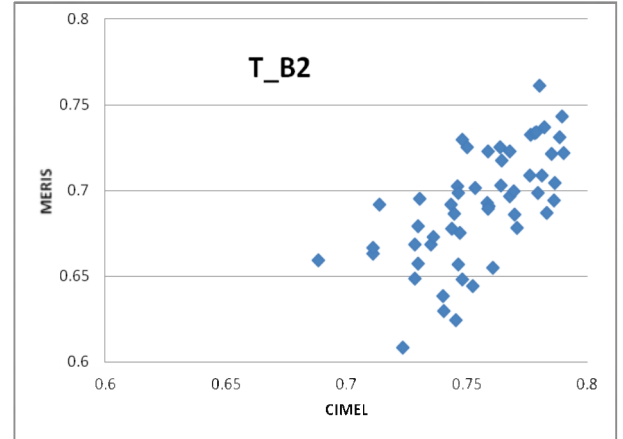
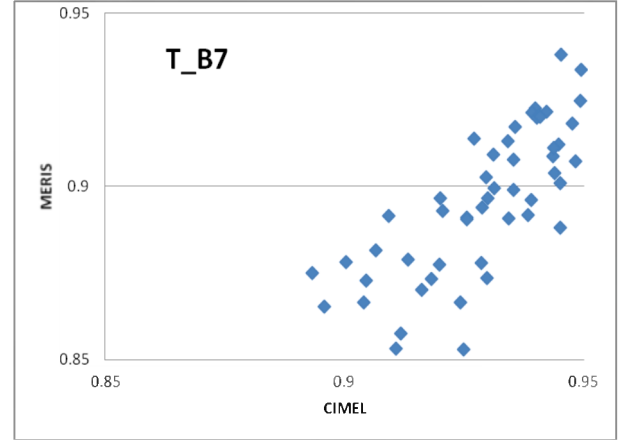
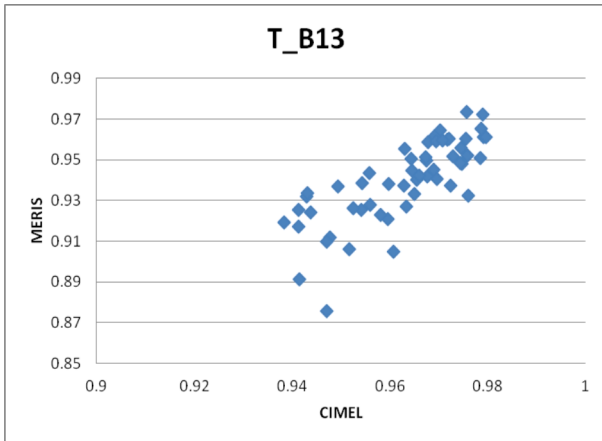


Figure 9: Aerosols transmittance at 443, 665 and 865 nm: comparison between MERIS and SOS simulations.

5 COMPARISONS ON THE WATER REFLECTANCE

5.1 Inter comparison MERIS L2 and CIMEL

The 5S formalism is used to perform the atmospheric correction. The MERIS input is the MERMAID TOA reflectance after correction for the sun glint and for the gaseous absorption. The atmospheric functions are computed as described previously. The water reflectance is deduced using Eq. 2;

The comparison in MERIS B_7 suggests that MEGS slightly over-corrects (Figure 10).

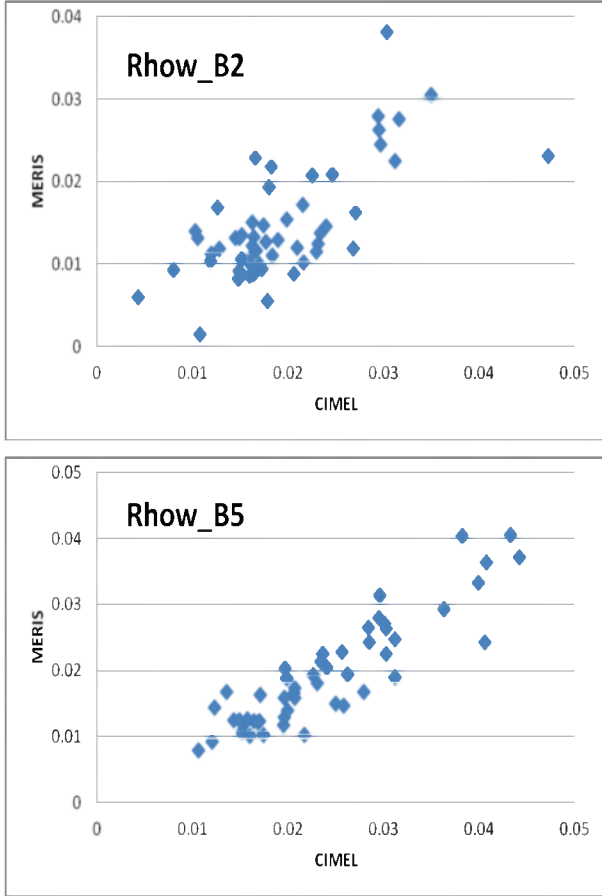


Figure 10: Water reflectance at 665 nm: comparison between MERIS and SOS simulations.

Table 1 provides the parameter of a linear fit on Figure 10 going through (0,0). The use of the ground-based aerosol measurements results in higher values of the water reflectance than MERIS. They are not correlated in the blue.

	B1	B2	B3	B4	B5	B6	B7
slope	0.58	0.74	0.83	0.83	0.84	0.57	0.47
R2	-0.10	0.38	0.73	0.79	0.86	0.54	0.35

Table 1: Water reflectance; slope and correlation factor for a linear regression.

Table 2 is identical to Table 1 except than we force the agreement in B_{13} on ρ_{aer} between the MERIS and CIMEL retrieval. The comparison is better except in B_1 where it is difficult to conclude anything with a non-correlation between the two sets.

	B1	B2	B3	B4	B5	B6	B7
slope	0.48	0.82	0.92	0.91	0.93	0.78	0.77
R ²	-1.66	0.28	0.63	0.77	0.90	0.74	0.71

Table 2: Same as Table 1 after adjustment in B_{13} .

5.2 MERIS L2 and CIMEL compared to *in situ* water reflectance measurements

We now use the *in situ* water reflectance measurements for comparison to MERIS L2 as well as to the AC we applied based on CIMEL and the SOS code. The comparison is on the normalized value. The BRDF correction on the SOS is the same than for MERIS L2. Figure 11 and Table 3 give the comparison in B_5 and B_2 . The correlation with *in situ* is weak and may need some filtering before any conclusion.

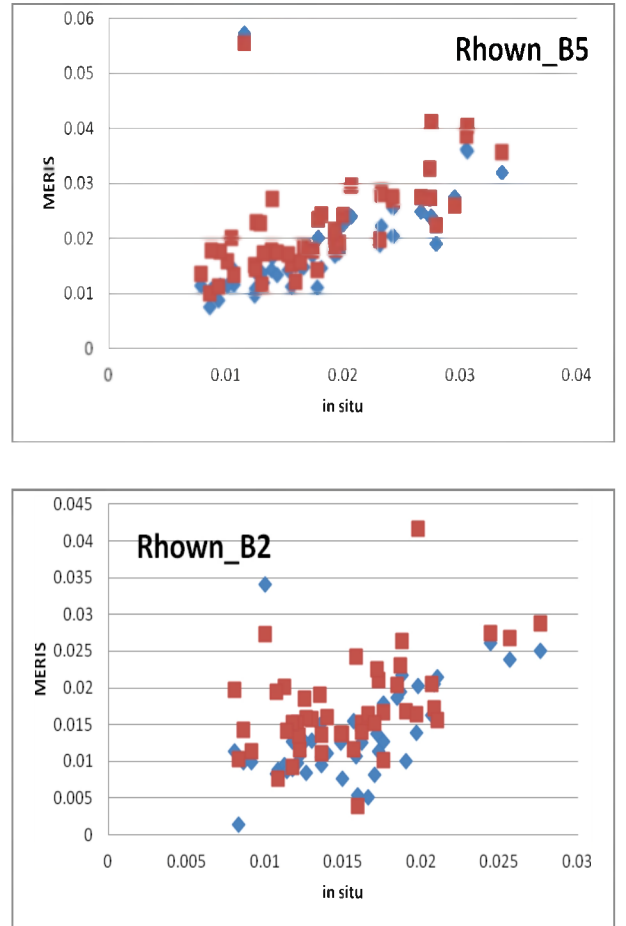


Figure 11: Water reflectance in B_5 and B_2 .

	B1	B2	B3	B5	B7
mean	0.69	0.87	0.97	0.99	0.88
R2	0.21	0.32	0.37	0.32	0.20
mean	0.94	1.09	1.15	1.18	1.55
R2	0.07	0.16	0.26	0.25	0.02

Table 3: Water reflectance; slope and correlation factor for a linear regression: MERIS L2 (upper values) and SOS (lower values).

5.3 Evaluation of the BPAC

We can also apply our own atmospheric correction in the NIR. The SOS ρ_{aer} is adjusted in B₁₃ to MERIS. We use the MERMAID BPAC [5] reflectance, on which we applied the atmospheric transmittance for a comparison in B₉ (Figure 12). The trend is there but with a large dispersion.

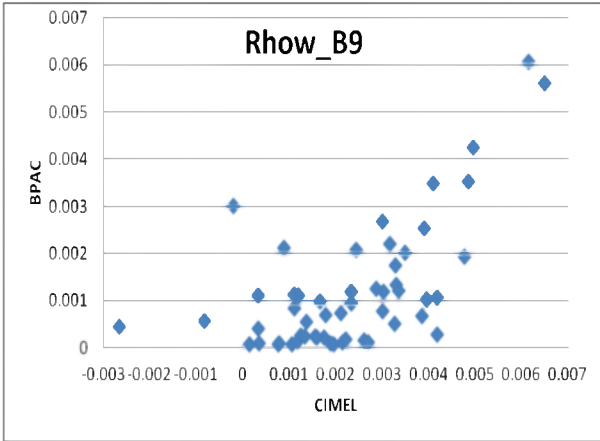


Figure 12: Water reflectance in B₉: comparison between BPAC and our approach.

6 CONCLUSIONS

We start the classical validation of the aerosol product through the use of the AOTs. The conclusions are well known with an overestimate of MERIS compared to AERONET.

We also use the CIMEL AOT when the medium glint flag is raised. The idea is to have a sun glint correction that includes the extinction by the aerosols. Clearly, when the medium glint flag is raised, we can disregard the MERIS L2 product. The clear recommendation is to have an aerosol remote sensing module that includes the direct-to-direct sun glint. This remark also applied to the introduction of the water reflectance in the NIR. It is not difficult to imagine a three spectral band algorithm that included all these parameters.

We proposed here a new approach to validate the atmospheric correction over water. This method is firstly based on the experimental determination of the aerosol IOPs thanks to AERONET. Secondly, we use the SOS radiative transfer code to predict at the time of MERIS overpass all the atmospheric functions required in the MEGS atmospheric correction procedure.

This protocol is applied here to the validation but it can be used as well for the vicarious calibration.

The results reported here, are more an illustration of the methodology than a quality assessment on the MERIS atmospheric corrections. This protocol should be validated and extended to the other AERONET Ocean Colour stations in order to make a significative analysis that separates the type of aerosols and the ranges of the scattering angle.

Because, it is an atmospheric approach we can also use the regular AERONET stations at sea without water reflectance measurements. Some of them are in small islands and the MERIS window can include them. Some are on the coast but if the aerosol model is spatially homogeneous, we can certainly use them: a readjustment on the aerosol reflectance in B₁₃ between MERIS and predicted will be applied. Anyway, we need to conduct an analysis on a large number of matchups first to be representative and second to subset for specific analysis (aerosol type, scattering geometry...)

As indicated in a companion paper [6], we have in mind to test the new aerosol models, and this approach of the validation can be used to evaluate the performances of the atmospheric corrections.

7 REFERENCES

- [1] Dubovik, O., and M. D. King, 2000. "A flexible inversion algorithm for retrieval of aerosol optical properties from Sun and sky radiance measurements", *Journal of Geophysical Research*, **105**: 20673–20696.
- [2] Deuzé, J.L., M. Herman, and R. Santer (1989), Fourier series expansion of the transfer equation in the atmosphere-ocean system, *Journal of Quantitative Spectroscopy & Radiative Transfer*, **41** (6), 483-494.
- [3] Santer, R., F. Zagolski, and O. Aznay, 2012. "Inherent optical properties of the aerosols for MERIS/OLCI-S3: From micro-physical properties to optical properties, *Proceedings of MERIS/AATSR & OLCI/SLSTR Preparatory Workshop*, Frascati (Italy), 15-19 October, 2012.
- [4] Cox, C., and W. Munk (1954), Measurements of roughness of the sea surface from photographs of the sun glitter, *Journal of Optical Society in America*, **44** (11), 838-888.

[5] Moore, G.F., Aiken, J. and Lavender, S.J., (2000), The Atmospheric correction of water colour and the quantitative retrieval of suspended particulate matter in Case II Waters: application to MERIS, Int. J. Rem. Sens.

[6] Zagolski, F., R. Santer, and O. Aznay, 2012. "Apparent optical properties of the aerosols for MERIS/OLCI-S3: Selection of the best LUTs for atmospheric correction over ocean, *Proceedings of MERIS/AATSR & OLCI/SLSTR Preparatory Workshop*, Frascati (Italy), 15-19 October, 2012.

ACKNOWLEDGMENTS

We thank G. Zibordi for the use of the AAOT AERONET data, the MERMAID team. This work was partially supported by the INTERREG 2 Seas program in the frame of the ISECA project.



Invest in our future